RSC Advances

PAPER

View Article Online
View Journal | View Issue

Cite this: *RSC Adv.*, 2017, **7**, 13919

The reactivity of Ti10Zr alloy in biological and electrochemical systems in the presence of chitosan

Vlad Gabriel Vasilescu,[a] Ion Sandu,[b] Gheorghe Nemtoi,[c] Andrei Victor Sandu,*[d] Vasilica Popescu,[e] Viorica Vasilache,[b] Ioan Gabriel Sandu[d] and Elisabeta Vasilescu[f]

This study presents a report on the electrochemical behavior of Ti10Zr, a material whose chemical composition (by lack of toxic elements in its composition) is highly controlled by its bio-compatibility, which is also recommended in oral implant dentistry. There has been an evaluation of the behavioral characteristics of the alloy within biological systems, such as the normal saline solutions (SF) and acid Ringer solutions (RAS), in the presence and absence of high level chitosan nano dispersions (CH) and a low level of polymerization (CL), respectively. The electrode processes within the two reference solutions (the saliva and the acid solution) led to the interface of the nanostructural rebuild, in the presence of chitosan dispersion, by obtaining an oxide and nanostructural oxy-hydroxy film (usually a mono-layer) with a passivating activity. The cyclic voltammograms indicated the fact that at the end of a 24 hour immersion in SF, bio-alloy Ti10Zr is already passivated, giving rise to a quasi-reversible oxidation–reduction process in the chitosan media in acetic acid solution. The evaluation of corrosion parameters (for example, the speed of corrosion, v_{cor} and resistance to polarization, R_p) of the potentiodynamic polarization curves, shows that the alloy Ti10Zr is highly stable in the studied media. After the immediate immersion of the bio-alloy, its speed of corrosion grows as follows: SF < RAS < CL < CH; 24 hours after the immersion of the alloy, passivation takes place and the aggression of the media studied increases in the order SF < CL < RAS < CH. The high resistance to corrosion of the bio-alloy Ti10Zr, was also confirmed by electrochemical impedance spectroscopy. The morphology of structures studied by scanning electron microscopy (SEM), indicates some specific modifications, and correlate very well with the data obtained by cyclic voltammetry (CV) as well as linear voltammetry (LV), and electrochemical impedance spectroscopy.

Received 6th January 2017
Accepted 15th February 2017

DOI: 10.1039/c7ra00231a

rsc.li/rsc-advances

Introduction

The main groups of bio-compatible materials used in dental medicine contain polymers, ceramics and their composites. The bio-compatibility of dental materials depends on their composition as well as on the interactions at the oral cavity level. The response of the material to be implanted when applying force or the degrading effects of biological fluids may alter its compatibility.[1] Tissues react differently to implants, depending on the type of the bio-material used, and the mechanism of the tissue attachment depends on its response to the surface of the implant. Generally, corrosive materials generate a severely toxic reaction having the rejection of the material in the tissue as an effect. The nature of the reactions to the implant-tissue interface shows a clear distinction between the bio-inert, bio-tolerated and bio-active materials.

The metals and alloys used as implant materials are those which, on their surfaces, can form stable protective passivation films, which "close" the metals from the corrosive environment.[1]

Titanium, a biologically inert material is deemed ideal to the endo-osseous dentistry implants, given that, when it is in contact with a tissue environment, it inactivates quickly by building a fine resistant and protective layer of titanium oxides. The fine titanium oxide film (mono-oxide, bi-oxide, tri-oxide) that is formed almost spontaneously (in less than one second) on the surface, regenerates continuously, is resistant to corrosion and allows the bone to develop inside the implant.[1,2] The bone grows on the coarse surface of the titanium implant creating a solid connection with the surrounding bone by

[a]University of Medicine and Pharmacy "Carol Davila" of Bucharest, Romania
[b]Alexandru Ioan Cuza University, Department of Interdisciplinary Research, Science Field, ARHEOINVEST Interdisciplinary Platform, Iasi, Romania
[c]Alexandru Ioan Cuza University, Faculty of Chemistry, Iasi, Romania
[d]Gheorghe Asachi Technical University, Faculty of Materials Science and Engineering, Iasi, Romania. E-mail: sav@tuiasi.ro
[e]Gheorghe Asachi Technical University, Faculty of Textiles, Leather Engineering and Industrial Management, Iasi, Romania
[f]Dunărea de Jos University of Galați, Faculty of Engineering, Galați, Romania

osteointegration, achieving a rigid anchorage which offers stability to the implant. Titanium alloys are even better tolerated than pure titanium, since the oxide layer building up is higher (*ca.* 10–20 μm) and the resistance to corrosion can be improved upon by alloying it with molybdenum, zirconium, rhenium, niobium, chrome, and manganese. The best known is the alloy Ti4Al6V, which holds 6% Al and 4% V in its composition. Its frequent choice to perform dentistry implants is determined by a combination between the most numerous and the most favorable characteristics, which include the following: high resistance to corrosion, low elasticity module and a good capacity for osteo-integration.[2] The analyses of possible reactions upon long lasting contact of live tissues with titanium alloying elements, limit the use of other elements, such as vanadium, aluminum, cobalt and nickel.

On the other hand, given the fact that the interaction between human and bio-material tissues takes place at the level of the two components of the interface, the surface properties of the material to be implanted are of utmost importance.

The application of bioactive nanoparticles on the implant surface will, for instance, enable the connection between the implant and the tissue to be much more natural, and thus significantly increase the stability and implicitly, and the life span of the implant. Recently, regenerative medicine and tissue engineering techniques developed strategies to obtain synthetic structures currently called "scaffold", which allow cell adhesion, increase and migration, as well as a three-dimensional architecture organization (3-D), similar to the desired tissue. The "scaffold" polymer structure determines the 3-D morphology, favors cell survival, confers mechanical stability, tissue growth, helps build up tissue structure and is replaced by the generated structure to form a natural, normal tissue. Polymer conventional chemistry manufactures a series of structures, such as nanofibres of different diameters and surface morphologies, nanocomposites and other macromolecular structures, that allow a high fiber interconnectivity and alignment control, which is also capable of sustaining cell orientation and migration.[3–9] Fibrin is a natural polymer[10] that builds up during blood clotting and plays an important role in homeostasis and wound healing. Fibrin hydrogels containing heparin can slowly and controllably release growth factors, with heparin binding affinity, such as FGF-2.[10] Chitosan has a similar GAG (glycosaminoglycan) structure, due to which it was investigated in several tissue engineering studies. Chitosan is a linear polysaccharide based on D-glucosamine and *N*-acetyl-D-glucosamine.[11] This polysaccharide is derived from chitin, which builds the exoskeleton of arthropods. It is soluble in diluted acid solutions and it jellies with pH increase or with the content decrease of the solvent. The de-acetylating level is about 70–80%, with chitosan being a polymer in which the free NH_2 group prevails (when all amino groups are acetylated, then the polymer is called chitin). Chitosan derivatives were obtained by reticulation with gluten aldehyde or UV (ultraviolet) irradiation and thermal variations. Chitosan is exhausted by lysozyme, and its kinetics of exhaustion are inversely correlated to the crystallinity level, which in turn varies with the level of acetylation.[12] Fig. 1 presents the chemical structure of chitosan.

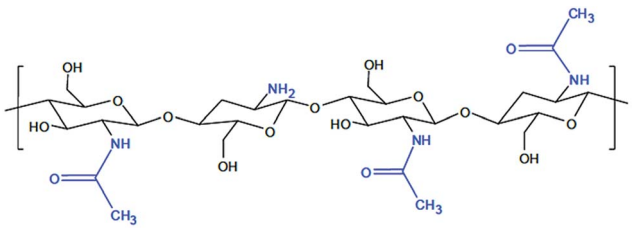

Fig. 1 Chemical structure of chitosan.[15]

The role of chitosan as a protective gel film with passivator activity of bio-compatible materials within the implantable systems is explained by using it as a colloid hydrogel. It is well known that the colloid stage is like that of a system with high dispersion, made up of fine particles, and characterized by a very large superficial surface. Together with the increase of the contact surface, the energy and reaction to the surface also increase. The hydrogel membrane structure built up on the surface of the alloy has a passivator role, which gives the alloy a different reactivity depending on its level of polymerization. With the low molar mass of chitosan nanodispersion, a thick gel film builds up, presenting low adhesion, while with the high molar mass of chitosan, the gel film is thin and adhesive and strongly passivating. The morphology of the structures formed on the surface of the alloy is influenced by the nature of the dispersion systems in which the corrosion tests take place, being strongly improved upon by passivation in the chitosan aqueous media, having certain characteristics.

The purpose of the research is to characterize the behavior towards electrochemical corrosion in the presence of chitosan bioalloy Ti10Zr. The results in this study complement those obtained in the study and the assessment of *in vitro* biocompatibility[13] of Ti10Zr, which is a material with high biocompatibility obtained by a strict control of the chemical composition (free from toxic elements, such as Al, V, Ni, Fe, *etc.* and elements present in titanium alloys frequently used in implant dentistry).[13–15]

This study reports, for the first time, the assessment of Ti10Zr alloy in the presence of chitosan for enhancing the behavior of the biocompatible alloy in different media, such as artificial saliva and other corrosive ones; the aspects considered in this study are not presented to date in literature, and this study represents a step forward for the use of chitosan in similar cases.

Materials and methods

The study used 5 Ti10Zr samples as tablet-like electrodes with a diameter of 20 mm and a height of 3 mm, incorporated into the epoxy resin, with a finely polished inner surface and the upper surface connected to an isolated copper collector wire. This alloy was developed, elaborated and characterized by the team, using the infrastructure of our laboratories from Dunărea

de Jos University of Galați, Gheorghe Asachi Technical University of Iasi and Alexandru Ioan Cuza University of Iasi.

Electrochemical behavior

All experiments were performed at room temperature (25 °C ± 1 °C) using an electrochemical cell with 3 electrodes connected to the PG STAT 302N (Metrohm-Autolab) Potentiostat Autolab, Nova 1.11 software. The reference electrode was one of silver chloride (AgCl), to which the values of potentials shall be referred to as the auxiliary platinum electrode, and the working electrode (Ti10Zr) were rebuilt by use of the material based on implant dentistry titanium. The following solutions were used as media:

(a). Low molar mass chitosan (30 000–50 000 g mol^{-1}) in aqueous acetyl acid solution (CL-chitosan low);

(b). High molar mass chitosan (190 000–410 000 g mol^{-1}) in aqueous acetyl acid solution (CH-chitosan high)

(c). Normal saline solution (SF), 0.1538 M NaCl (0.9% grav.)

(d). Acid Ringer solution with sulphuric acid (RAS), with pH = 1.00.

For the electrochemical studies, the 2 M acetate lock was used to determine the influence of acetic acid on voltammetric behavior by comparing it with that of the chitosan solutions. For pH determination, an electric conductivity Consort 861 electrochemical multi-meter was used. Electrochemical measurements are recommended due to their simplicity and speed when compared with others, and it is also due to the fact that these measurements can provide significant amount of information on the quality of the electrochemical measurements as well as the quality within the study of the corrosion process, and they are generally non-invasive.[16–20]

EDX analysis

Following the corrosion tests, the 5 samples were analyzed with a scanning electron microscope, SEM, coupled to an EDX detector, with a view of determining the chemical composition of the elements in the analyzed surfaces. The analysis of the samples (composition and microstructural morphology) was carried out using a scanning electron microscope (SEM), model VEGA II LSH, produced by TESCAN Czech Republic, coupled with an EDX QUANTAX QX2 detector, manufactured by BRUKER/ROENTEC Germany. Sample analysis was performed at a range between 200 and 2500× magnification with an accelerating voltage of 30 kV, and the working pressure was less than 1×10^{-2} Pa. The resulting image was formed by Secondary Electrons (SE) and Backscatter Electrons (BSE).

Results

Characterization of the electrochemical behavior

The low (CL) and high (CH) molar mass of chitosan solutions of 2% were prepared in aqueous solutions of 6.5% acetic acid and the pH was 2.67 and 2.62, respectively, and the electroconductivities, κ, were 1712 μS cm^{-1} and 2180 μS cm^{-1}, respectively. Fig. 2a presents cyclic voltammograms (CV)

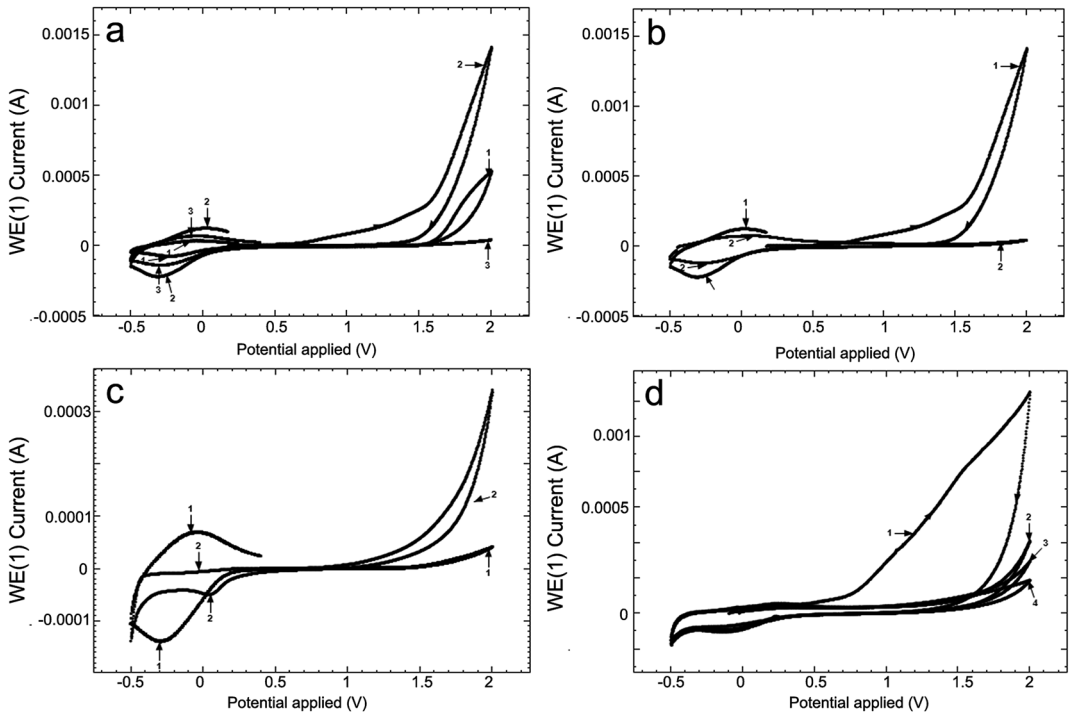

Fig. 2 Cyclic voltammograms (CV) for (a) Ti10Zr alloy at 100 mV s^{-1} in (1) CL, (2) CH, (3) acetate lock (AL); (b) Ti10Zr in ChitHigh immediately after immersion (1) and 4 days after immersion (2); (c) in acetate lock on Ti10Zr (1) and on Pt (2); (d) in acid medium (pH = 1.00) at different moments after immersion: (1) immediately after immersion, (2) at 5 minutes after immersion, (3) at 80 minutes after immersion, (4) at 17 hours after immersion.

Table 1 The parameters obtained by means of the cyclic voltammograms (CV) of Ti10Zr in chitosan and acetate lock media

Medium	E_{pa}, V	I_{pa}, μA	E_{pc}, V	$-I_{pc}$, μA	E_{transp}, V	E_{repas}, V
Chitosan low (CL)	−0.067	40	−0.240	71	1.559	1.576
Chitosan high (CH)	0.023	129	−0.304	217	0.624	1.372
Acetate lock (AL)	−0.026	68	−0.288	140	1.616	1.670

obtained in the 2 chitosan solutions (curves 1 and 2) and in 2 M acetate lock (curve 3) of the studied alloy Ti10Zr.

Table 1 presents the parameters obtained by means of the cyclic voltammograms (CV) of Ti10Zr in chitosan and acetate lock media from Fig. 2a.

Fig. 2b presents the cyclic voltammograms (CV) of alloy Ti10Zr in ChitHigh immediately after immersion and, again, 4 days after immersion. Moreover, Fig. 2c shows the cyclic voltammograms (CV) in acetate lock on Ti10Zr and on Pt. Cyclic voltammograms (CV) were obtained in the acid medium (pH = 1.00) at different moments after immersion, which were considered important for further evaluation and correlation with other data (Fig. 2d).

Fig. 3 presents cyclic voltammograms of the 4th medium, the 3 previously mentioned media and the 4th being a normal saline solution (SF), at a scanning speed of 100 mV s^{-1}, immediately after immersion (Fig. 3a) and 24 hours after immersion (Fig. 3b).

In order to compare the surface effect of the 4 media (CL, CH, SF and RAS) on the alloy, the linear voltammetry (LV) studies, at a scanning speed of 50 mV s^{-1}, at 24 hours (Fig. 4) were carried out.

Based on the data obtained from potentio dynamic polarization curves, using the Nova 1.11 software corrosion, we obtained the Tafel indices (b_a and b_c), corrosion potential, (E_{cor}) defined as the intersection of the Tafel lines (anodic and cathodic branch), the density of the corrosion current (j_{cor}), corrosion speed (v_{cor}) and polarity resistance (R_p),[21–24] presented

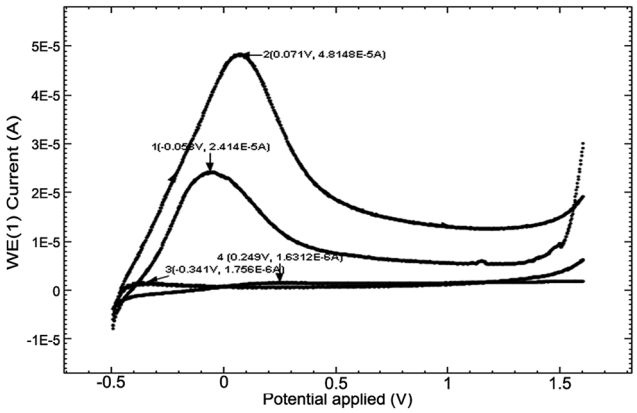

Fig. 4 Linear voltammetry (LV) for the 4 media, at scanning speeds of 50 mV s^{-1}, at 24 hours following the immersion: (1) CL, (2) CH, (3) SF and (4) RAS of alloy Ti10Zr.

in Table 2. When calculating the corrosion speed, current density, j, was taken into account, which can be defined by the Butler–Volmer relation:[25]

$$j = j_{cor}\left[\exp\left(\frac{2.303(E-E_{cor})}{b_a}\right) - \exp\left(-\frac{2.303(E-E_{cor})}{b_c}\right)\right] \quad (1)$$

where b_a and b_c are the Tafel slopes:

$$b_a = \frac{RT}{\alpha nF} \text{ and } b_c = \frac{RT}{(1-\alpha)nF} \quad (2)$$

The potential scanning speed was 0.5 mV s^{-1}, on field PCD ± 0.100 V, and the Tafel parameters for the envisaged 4 media where the working electrode surface (Ti10Zr) was of 2.5434 cm^2, are given in Table 2.

Electrochemical impedance spectroscopy (EIS) was used to characterize the behavior of Ti10Zr in the 4 media. The spectra were set immediately after the immersion of the alloy in each of the media and the stationary status in the system was reached (with potential within an open circuit) and then, at 24 hours after immersion. The equivalent circuit (Fig. 5), which behaved best in taking over the experimental data,[26] obtained

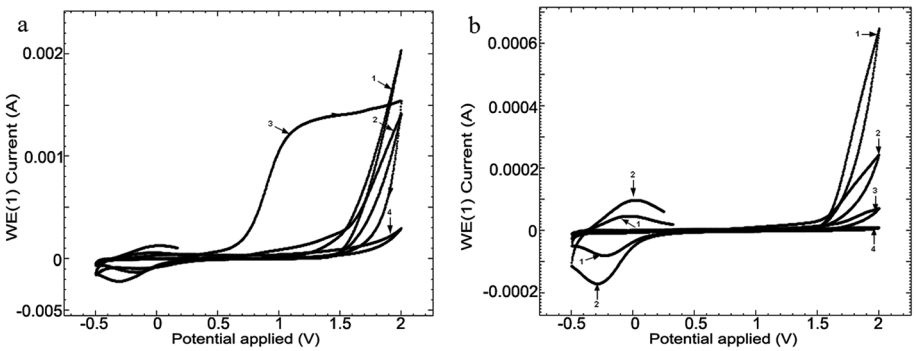

Fig. 3 Cyclic voltammograms (CV) obtained in the 4 media when immersing Ti10Zr (a) and after 24 hours after immersion (b): CL (1), CH (2), SF (3) and RAS (4), at a scanning speed of 100 mV s^{-1}. The pitting corrosion of Ti10Zr immersed in the 4 media shows up only in SF at high potentials, in the field: 2.73–3.00 V.

Table 2 Corrosion parameters of the Ti19Zr samples in the envisaged media

	b_a (mV dec^{-1})	b_c (mV dec^{-1})	E_{cor} (mV)	j_{cor} (nA cm^{-2})	v_{cor} (μm per year)	10^{-3} R_p (Ω)
Immediately after immersion						
CL	51.4	220.4	253.2	7.04	0.061	1011.0
CH	25.6	171.0	59.0	34.77	0.303	109.5
SF	241.4	35.9	−261.2	2.89	0.025	1327.0
RAS	86.4	69.0	−114.0	6.28	0.055	1058.0
24 Hours following the immersion						
CL	146.9	15.8	184.8	2.77	0.024	879.0
CH	366.2	15.3	107.5	15.29	0.133	163.7
SF	255.3	36.6	40.1	2.96	0.026	1847.0
RAS	102.5	201.4	201.1	11.35	0.088	1022.0

for Ti10Zr in the 4 media by electrochemical impedance spectroscopy (EIS), was R (RQ): the first R, (R_s), representing the ohmic fall within the solution or the non-compensated resistance, the second R, (R_p), is the resistance to polarity and Q is the constant phase element (CPE) defined by the following relation:

$$Z_{CPE} = \frac{1}{Y_0(j\omega)^N} \quad (3)$$

where Y_0 is the admittance, ω is the angular frequency of the alternative current, $j = (-1)^{1/2}$ and N is the exponent of the constant phase element.

The obtained Nyquist diagrams for the open circuit potential, at an amplitude of the alternative current of 10 mV and in the frequency range of 10^{-1} to 10^5 Hz are presented in Fig. 6.

Table 3 also presents the parameters obtained by the EIS, that resulted from the Nyquist and Bode diagrams.[27,28]

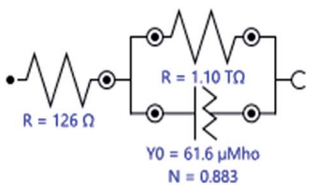

Fig. 5 The equivalent circuit used to process experimental data by EIS, upon immersion of the alloy sample Ti10Zr in CL.

SEM-EDX analysis

Fig. 7 presents the EDX spectra and the microphotographs of the analyzed surfaces of the five samples: benchmark (reference), CL (chitosan low), CH (chitosan high), SF (normal saline

Table 3 Experimental data obtained by EIS for alloy Ti10Zr

Medium	CPE, μMho	N	R_s, Ω	φ, °
Immediately after immersion				
CL	61.6	0.883	126	79
CH	165	0.742	144	66
SF	25.4	0.890	18	80
RAS	385	0.778	7	70
At 24 hours after immersion				
CL	215	0.708	81.4	63
CH	182	0.605	74.2	54
SF	24	0.864	21.1	78
RAS	276	0.743	6.6	67

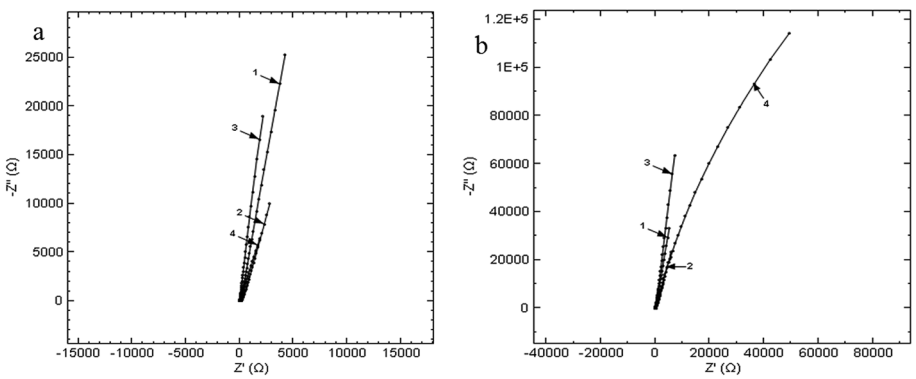

Fig. 6 Nyquist diagrams at immersion (a) and after keeping the Ti10Zr for 24 hours (b), in the 4 media, on the frequency range 0.1 ÷ 10^5 Hz la PCD: (1) CL, (2) CH, (3) SF and (4) RAS.

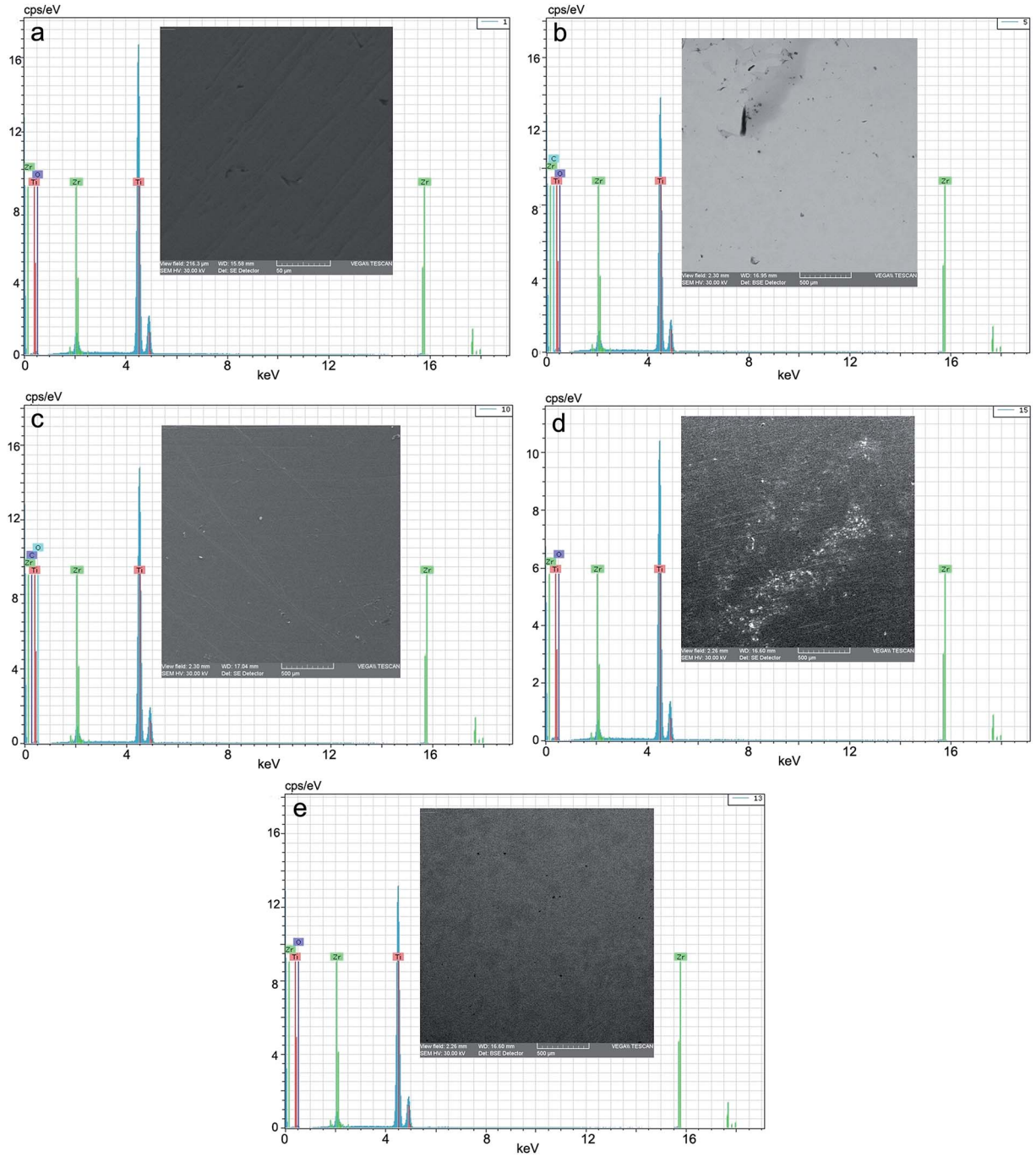

Fig. 7 EDX spectrum and microphotograph of the electrode surface: (a) benchmark/reference; (b) after corrosion in CL, (c) after corrosion in CH, (d) after corrosion in SF, (e) after corrosion in RAS.

solution) and RAS (Ringer solution, acidulated with sulphuric acid, pH = 1.00).

Discussion

Characterization of the electrochemical behavior

Fig. 2 shows the influence of different parameters on the peak currents (anode and cathode) and more specifically, the influence of the environment. The cyclic voltammograms in Fig. 2 indicated a quasi-reversible redox process due to the acetic acid in the potential field −0.4 to 0.0 V; the currents of the reduction and oxidation (I_{pc} and I_{pa}) increase as follows: CL < acetate lock (AL) < CH, while the transpassivation and repassivation potentials decrease as follows: AL > CL > CH, as can be seen from Table 1.

Of these 3 media, the most reactive to support (alloy Ti10Zr) is ChitHigh (CH). Keeping the alloy immersed for a long time in this medium, the passivation showed in Fig. 2b takes place,

where the cyclic voltammograms (CV) are shown at 4 days after the immersion (curve 2) by comparison with that obtained immediately after immersion (curve 1).

While comparing the CV obtained in the acetate lock on Ti10Zr and on Pt (Fig. 2b) we noticed that the oxidation of the acetic acid in the dispersion medium takes place only on alloy Ti10Zr, while only the reduction of the acetic acid takes place on the electrode on Pt (the oxidation process of the acetic acid being catalyzed on the titanium alloy, which is much more resistant to corrosion in the acetate medium than Pt), as shown in Fig. 2c (CV-1).

The behavior of bioalloy Ti10Zr in the acid medium with pH = 1.00 (following the immersion of the alloy) as indicated by the cyclic voltammograms (CV) shows its reactivity even at a rather low potential (0.72 V). After keeping it in this medium for as short a time as 5 minutes, the alloy is passivated, and the passivation is amplified with time (Fig. 2d).

The cyclic voltammograms of all the 4 media in the mentioned field supported the fact that in SF, Ti10Zr initially presents a lower resistance to corrosion, but after 24 hours, the material is already passivated, still continuing a quasi-reversible redox process in the chitosan media in acetic acid solution due to the effect of the acetic acid, as shown in Fig. 3b (drops 1 and 2 corresponding to the curves bearing the same numbers).[29–31]

Linear voltammetry also showed the quasi-reversible redox process in the chitosan media with acetic acid on Ti10Zr, which confirms all that has been mentioned concerning the catalytic action of the alloy in acetic acid electro-oxidation, and the alloy passivation in the media envisaged after 24 hours following the immersion (Fig. 4).

The corrosion speed (v_{cor}) as well as the resistance to polarity (R_p) shows that alloy Ti10Zr is highly stable in the envisaged media, the corrosion speed at immersion increased in the following order: SF < RAS < CL < CH. After 24 hours, the passivation of the alloy takes place, the corrosion speed decreases with time, and the aggression of the media also increases in the following order: SF < CL < RAS < CH; corrosion speeds in CL and RAS are very close, yet the change in order concerning the aggression of the two media suggests that alloy passivation is more prevalent in CL.

The parameter N of the constant phase element is associated with the uneven distribution of current due to roughness and surface flaws. Factor N is also known as roughness coefficient and can be calculated as being the linear part of the Bode representation.[32] When $n = 1$, the constant phase element describes an ideal capacitor, when $n = 0$ it describes a resistor, and when $n = -1$ it refers to an inductor. Generally, corroded surfaces have $n = 0.8$ for uneven corrosion, $n = 0.6$–0.7 for general uneven corrosion and $n = 0.4$–0.5 for spotted corrosion or pitting corrosion.[33]

The high resistance to corrosion of Ti10Zr is also indicated by the electrochemical impedance spectroscopy demonstrated immediately after immersion, as well as at 24 hours after immersion in the 4 media used, while the value of the polarity resistance exceeds 1000 GΩ (1.10 TΩ).

The presence of the constant phase element shows the roughness and porosity of the electrode or the uneven distribution of the electroactive species, and the passive film built up on the surface of the electrode to be compact if the phase angle (φ) is close to 90°. According to the values of φ and N in Table 3, we could say that upon the initial immersion of Ti10Zr in the 4 media, the corrosion of the bio-material is even, which corresponds with the cyclic voltammetry, and at 24 hours after immersion, there is a general uneven corrosion only in CH, the corrosion process being even in the other media.

The value of the polarity resistance obtained by EIS is much higher than those calculated by the potentio dynamic polarization curves due to the different time of immersion to achieve the stationary stage and to reach PCD, as well as for the time necessary to lay the EIS spectra. The presence of acetate ions in the chitosan media protects the surface of the implantable biomaterial, (alloy Ti10Zr) which plays a catalytic role within the oxidation process of the acetic acid, and the resistance to corrosion of this alloy is much better than that of pure Ti.[22,31]

In conclusion, we could say that based on the electrochemical determinations, alloy Ti10Zr presents a very good resistance to corrosion, and the introduction of Zr improves the qualities of Ti even more. In the acetic acid with chitosan media, we noticed the occurrence of an oxidation process of the acetic acid, which protects the surface of the alloy, coupled with a reduction process. On Pt, in the acetic acid medium, the reduction process is well shaped (there is no oxidation of it), which indicates the special qualities of the studied alloy – Ti10Zr.

SEM-EDX analysis

The morphology of the structures on the surface of the alloy, analyzed by scanning electron microscopy, showed some specific modifications depending on the nature of the dispersion systems, in which the corrosion tests were performed. These correlate very well with the data obtained by cyclic voltammetry (CV) and linear voltammetry (LV), as well as by EIS. Thus, by comparison with the benchmark (Fig. 7a) the morphology of the corrosion structures is highly improved by passivation in the two other aqueous chitosan dispersions (Fig. 7b and c) and highly activated in normal saline solution and Ringer solution acidulated with sulphuric acid, at pH = 1.00 (Fig. 7d and e). In Ringer solution, grading and distribution of the crystals of the corrosion products is even; in normal saline solution, there emerged areas of products with smaller grading and uneven distributions.

The presence of chitosan in the immersion aqueous system (acetic acid), by the hydrogel membrane-like structure, built up *in situ* on the surface of the alloy as a protective gel film, plays a passivator role. This confers a different reactivity to the alloy, depending on its level of polymerization. In the low molar mass of chitosan nanodispersion (30 000–50 000 g mol^{-1}), a thick gel film with low adhesion (Fig. 7c) forms, while in that with high molar mass (190 000–410 000 g mol^{-1}), the gel film is thin and adhesive, as well as highly passivating (Fig. 7d).

With regard to the chemical composition (Table 4), in the assessment of the EDX spectra, the data are only informative, and are relatively different from the spectral data.

For behavioral studies on corrosion, the chemical composition data were reported to the benchmark or reference sample,

Table 4 EDX analysis of the surfaces after the corrosion test

Samples	Element	Weight, %	Atomic, %	Error, %
Etalon	Titanium	90.066	94.528	3.244
	Zirconium	9.934	5.472	0.551
SF	Titanium	90.088	94.540	3.159
	Zirconium	9.912	5.460	0.600
RAS	Titanium	89.739	94.338	3.188
	Zirconium	10.261	5.662	0.615
CL	Titanium	77.838	62.401	2.738
	Zirconium	8.005	3.368	0.495
	Carbon	0.336	1.075	0.148
	Oxygen	13.820	33.156	40.707
CH	Titanium	81.216	69.451	3.196
	Zirconium	8.398	3.769	0.536
	Carbon	0.238	0.812	0.129
	Oxygen	10.148	25.968	36.417

and thus, we can notice that in normal saline solution, the composition in Zr decreases very little, detriment to Ti, while in Ringer solutions, conversely, the composition in zirconium increases detrimentally to titanium. In the case of two chitosan dispersions, the elementary composition clearly shows the difference between the two gel films built up on the surface of the alloy; the one with low molar mass submitted in high concentration, by comparison to the one with high molar mass submitted in a lower concentration (thin layer).

Conclusions

The electrochemical determinations show the fact that bioalloy Ti10Zr presents a very good resistance to corrosion in the studied media, the introduction of Zr is noted to highly improve the qualities of Ti. Other conclusions derived from the research performed are follows:

- In the presence of chitosan dispersion, a protective gel film with passivating activity results *in situ*. The presence of acetate ions in chitosan media protects the surface of the implantable bio-material (alloy Ti10Zr), which plays a catalytic role in the oxidation process of the acetic acid, and the resistance to corrosion of this bio-alloy is much better than that of a pure Ti. On Pt, in an acetic acid medium, the reduction process is well defined (its oxidation does not occur), which shows the special qualities of the studied alloy, Ti10Zr.

- By cyclic voltammetry, linear voltammetry and EIS, we showed that bio-alloy Ti10Zr is highly stable in the envisaged media, following immediate immersion when the corrosion speed increased as follows: SF < RAS < CL < CH. At 24 hours from immersion, the passivation of the alloy occurs, the corrosion speed decreases with time, and the aggression of the envisaged media increases as follows: SF < CL < RAS < CH; the corrosion speeds in CL and RAS are very close, yet the change of order concerning the aggression of the two media suggests the fact that the passivation of the alloy in CL is more important.

- The presence of chitosan in the immersion aqueous system, low acid (acetic acid), by the hydrogel membrane-like structure, which built up *in situ* on the surface of the alloy in the shape of a protective gel film, plays a passivating role. This confers the alloy with a different reactivity, depending on its level of polymerization. In low molar mass (30 000–50 000 g mol^{-1}) chitosan nanodispersion, we noticed the formation of a thick, low adhesive gel film, while with the high molar mass (190 000–410 000 g mol^{-1}), the gel film is thin and adhesive, as well as highly passivating.

- The assessment on EDX spectra of the chemical composition shows the fact that in a normal saline solution, the content of Zr decreases very little detrimentally to Ti, but in Ringer solutions, the zirconium content increases. In the case of the two chitosan dispersions, the elementary composition shows clearly the difference between the two gel films built up on the surface of the alloy, the low molar mass submitted into a higher concentration, in opposition to the one with high molar mass submitted into a lower concentration (thin layer).

References

1 E. Vasilescu and V. G. Vasilescu, *Studies on the biocompatibility of titanium based alloys used in oral implantology, International Conference of Young Researchers New Trends in Environmental and Materials Engineering*, TEME, Galati, Romania, 2013.
2 H. J. Song, S. H. Park, S. H. Jeong and Y. J. Park, *J. Mater. Process. Technol.*, 2009, **209**, 864.
3 S. F. Badylak, *Semin. Cell Dev. Biol.*, 2002, **13**, 377–383.
4 D. S. Kohane and R. Langer, *Pediatr. Res.*, 2008, **63**, 487–491.
5 K. Gelse, E. Poschl and T. Aigne, *Adv. Drug Delivery Rev.*, 2003, **55**, 1531–1546.
6 T. Hanawa and M. Ota, *Biomaterials*, 1991, **12**, 767–774.
7 U. Hersel, C. Dahmen and H. Kessler, *Biomaterials*, 2003, **24**, 4385–4415.
8 J. Hodd, R. Record, R. Tullius and S. Badyak, *Biomaterials*, 2002, **23**, 1841–1848.
9 S. J. Peter, M. J. Miller, A. W. Yasko, M. J. Yaszemski and A. G. Mikos, *J. Biomed. Mater. Res.*, 1998, **43**, 422–427.
10 L. J. Currie, J. R. Sharpe and R. Martin, *Plast. Reconstr. Surg.*, 2001, **108**, 1713–1726.
11 V. K. Mourya and N. Inamdar, *React. Funct. Polym.*, 2008, **68**, 1013–1051.
12 J. L. Drury and D. J. Mooney, *Biomaterials*, 2003, **24**, 4337–4351.
13 V. G. Vasilescu, M. S. Stan, I. Patrascu, A. Dinischiotu and E. Vasilescu, *Rom. J. Morphol. Embryol.*, 2015, **4**, 240–246.
14 V. G. Vasilescu, I. Patrascu, C. Cosmin and E. Vasilescu, *Rev. Chim.*, 2016, **67**, 263–266.
15 H. P. Wiesmann, N. Nazer, C. Klatt, T. Szuwart and U. Meyer, *J. Oral Maxillofac. Surg.*, 2003, **61**, 1455–1462.
16 G. Nemtoi, M. S. Secula, I. Cretescu and S. Petrescu, *Rev. Chim.*, 2007, **58**, 1216–1220.
17 S. Petrescu, M. S. Secula, G. Nemtoi and I. Cretescu, *Rev. Chim.*, 2009, **60**, 462–467.
18 A. V. Sandu, A. Ciomaga, G. Nemtoi, C. Bejenariu and I. Sandu, *Microsc. Res. Tech.*, 2012, **75**, 1711–1716.

19 G. Nemtoi, F. Ionica, F. Lupascu and A. Cecal, *Chem. J. Mold.*, 2010, **5**, 98–105.
20 A. V. Sandu, A. Ciomaga, G. Nemtoi, M. M. A. B. Abdullah and I. Sandu, *Instrum. Sci. Technol.*, 2015, **43**, 545–557.
21 S. Ningshen, U. Kamachi Mudali, G. Amarendra and R. Baldeo, *Corros. Sci.*, 2009, **51**, 322–329.
22 D. M. Gordin, T. Gloriant, F. Nemtoi, R. Chelariu, N. Aelenei, A. Guillou and D. Ansel, *Mater. Lett.*, 2005, **59**, 2936–2941.
23 G. Nemtoi, A. Ciomaga and T. Lupaşcu, *Rev. Roum. Chim.*, 2012, **57**, 837–841.
24 Q. Guo, J. H. Liu, M. Yu and S. M. Li, *Acta Metall. Sin.*, 2015, **28**, 139–146.
25 D. A. Jones, *Principles and prevention of Corrosion*. Macmillan, New York, 1992.
26 B. A. Boukamp, *Solid State Ionics*, 1986, **20**, 31–44.
27 N. Mahato and M. M. Singh, *Port. Electrochim. Acta*, 2011, **29**, 233–251.
28 Z. Yao, Z. Jiang and F. Wang, *Electrochim. Acta*, 2007, **52**, 4539–4546.
29 A. V. Sandu, A. Ciomaga, G. Nemtoi, C. Bejenariu and I. Sandu, *J. Optoelectron. Adv. Mater.*, 2012, **14**, 704–708.
30 M. Sànchez, J. Gegori, M. C. Alonso, J. J. Garcia-Jareno, H. Takenouti and V. Vicente, *Electrochim. Acta*, 2007, **52**, 7634–7641.
31 D. Mareci, C. Bocanu, G. Nemtoi and D. Aelenei, *J. Serb. Chem. Soc.*, 2005, **70**, 891–897.
32 J. R. Macdonald and W. B. Johnson, *Fundamentals of Impedance Spectroscopy*, John Wiley and Sons, 2005.
33 J. R. Macdonald, *Ann. Biomed. Eng.*, 1992, **20**, 289–305.